J. Fluid Mech. (1978), *vol.* 88, *part* 3, *pp.* 465–483
Printed in Great Britain

Entry flow in a heated straight tube

By LUN-SHIN YAO
The Rand Corporation, Santa Monica, California†

(Received 9 August 1977)

The developing flow in the entry region of a heated horizontal pipe is analysed. The asymptotic solution of the developing flow near the entrance of the heated straight pipe, distance $O(a)$, is obtained by perturbing the solution of the developing flow in an unheated straight pipe. Two vortices result from the combination of the radial-directional and the downward motions of the fluid particles which are induced by the displacement of the boundary layer and develop along the pipe. The axial velocity has a concave profile in the inviscid core with its maximum off the centre-line near the entrance and it grows toward a uniformly distributed profile downstream. The downward stream caused by the displacement of the secondary boundary layer forces the axial velocity profile to turn anticlockwise continuously along the pipe if the flow is from left to right. The core flow induced by the axial boundary-layer displacement generates a favourable pressure gradient. Simultaneously, the secondary boundary-layer displacement affects the core flow to induce a favourable pressure gradient on the bottom of the pipe and an unfavourable pressure gradient on the top wall. The effect of the axial boundary-layer displacement is stronger than that of the secondary boundary layer near to the entrance. Downstream the growth of the boundary-layer thickness is suppressed by the inviscid secondary flow. It is expected that the displacement effect of the secondary boundary layer becomes dominant downstream from the region of $O(a)$ when Gr is large.

1. Introduction

The entry developing flow in pipes has been of great importance in a number of engineering devices. Also, it has attracted many researchers' interests because it is a standard problem in laminar-flow theory (see Yao 1977).

In this paper we study the entry-developing flow in a heated straight pipe under the conditions of constant wall heat flux. The solution is valid within the distance $O(a)$ from the pipe entrance. The inlet velocity W_{in} is uniformly distributed. The wall of the pipe is maintained at the constant heat flux q_w. The governing parameters of the problem are [see (2)]:

$$\left.\begin{aligned} &\text{(i) the Reynolds number} && Re = \frac{W_{\text{in}} a}{\nu}, \\ &\text{(ii) the Grashof number} && Gr = \frac{\gamma g a^4 q_w}{k\nu^2}, \\ &\text{(iii) the Prandtl number} && Pr = \frac{\nu}{\kappa}, \\ &\text{(iv) the ratio} && \epsilon = \frac{Gr}{Re^{\frac{5}{2}}} \text{ (constant wall heat flux),} \end{aligned}\right\} \tag{1}$$

† Present address: Department of Mechanical and Industrial Engineering, University of Illinois, Urbana, Illinois 61801.

where a is the radius of the pipe, ν is the kinematic viscosity, γ is the thermal expansion coefficient, g is the gravitational acceleration, κ is the thermal diffusivity, and k is the thermal conductivity.

The physical meaning of ϵ is the ratio of the buoyancy force and the viscous forces. It should be noted that when ϵ is small it does not necessarily imply that the heat transfer rate is small, because ϵ can be small when Re is large. It is also worth mentioning that the entry laminar flow is not restricted by the critical Reynolds number, $Re_{\text{critical}} = 1000$, of the fully developed flow in an unheated straight pipe. In other words, the entry flow can be laminar even when $Re > 1000$, but the flow transition may occur before it becomes fully developed.

The entry condition (velocity distribution) of a pipe flow has attracted substantial attention from the fluid mechanics community (see Van Dyke 1970; Wilson 1971; Smith 1976). Smith (1976) studied the transition of Poiseuille flow from a straight pipe into a curved one. However, the solution obtained by Smith is valid only for very small $\bar{\alpha}$, $\sim O(Re^{-2})$. Thus strong upstream influence of the curved pipe on the transition of the Poiseuille flow which was observed by Ito (1961) is not predicted in Smith's solution. There are two popular idealized entry conditions for the entry pipe flow problem: uniformly distributed axial velocity profile and Poiseuille flow. In reality, none of them can be obtained easily. Ideally, the Poiseuille flow might be obtained by connecting a long straight pipe to a curved pipe of the same diameter. However, owing to the strong upstream curvature effect, the flow starts to deviate from Poiseuille flow far upstream before the fluid gets into the curved pipe. Similar flow development can occur in a heated straight pipe. Therefore, in reality, Poiseuille flow cannot be obtained at the entrance of a curved pipe or a heated straight pipe. On the contrary, the uniformly distributed velocity can be achieved to a degree by connecting a rapid well-rounded contraction and boundary-layer suction ahead of the pipe entrance. This method was used by Agrawal, Talbot & Gong (1978) in their experimental study of the entry flow in curved pipes, and by Barker & Jennings (1977) in their study of the entry flow in a heated straight pipe.

In this paper, the idealized entry condition, a uniformly distributed axial velocity profile, is assumed to study the flow development in a heated straight pipe. The related works on the entry flow in an unheated straight pipe as well as in an unheated curved pipe are briefly reviewed before the discussion of the physics of the entry flow in a heated straight pipe.

Unheated straight pipes

Previous work on developing flow in unheated straight pipes or two-dimensional channels falls into the following four categories: (i) linearization of the momentum equations; (ii) two-zone models, in which a boundary-layer flow matches with the downstream perturbation solution for the fully developed flow; (iii) momentum-integral techniques; and (iv) finite-difference solutions. A detailed review of the published papers falling into the above four categories has been summarized by Yao & Berger (1975). From a critical analysis of the entry flow problem, Van Dyke (1970) pointed out that there are two length scales in channel entry flow: a, the half-width of the channel, and aRe. Most of the early work on this problem is only valid for downstream distance $O(aRe)$. Van Dyke obtained a solution in the upstream region, for distance $O(a)$, and so reconciled the discrepancy between the earlier theoretical results

and the experimental data near the entrance of the channel. Independently, a similar, but more detailed mathematical analysis was given by Wilson (1971).

Curved pipes

Two parameters govern the developing entry flow in curved pipes: $\bar{\alpha}$, the curvature ratio; $D = \bar{\alpha}^{\frac{1}{2}}Re$, the Dean number (Dean 1927, 1928). The curvature ratio $\bar{\alpha}$ is defined as the ratio of a and R, where R is the radius of curvature of the curved pipe; therefore, the value of $\bar{\alpha}$ cannot be larger than one. The influence of the centrifugal force on the entry flow development depends on the value of $\bar{\alpha}$. So far, there is not sufficient information to define for how small an $\bar{\alpha}$ Singh's solution (1974) is correct or for how large an $\bar{\alpha}$ Yao & Berger's solution (1975) is valid. This question can only be answered by comparing Singh's solution or Yao & Berger's solution with a numerical solution of the Navier–Stokes equations or a careful experimental measurement on many curved pipes of different $\bar{\alpha}$. Unfortunately, none of them are available. In the following discussion, the value of $\bar{\alpha}$ is defined in the asymptotic sense. When we say $\bar{\alpha}$ is small, it means that $\bar{\alpha}$ is only slightly larger than zero (Agrawal *et al.* (1978) showed experimentally that Singh's solution is not accurate when $\bar{\alpha} \geqslant 0{\cdot}05$); when $\bar{\alpha}$ is large, it means that the value of $\bar{\alpha}$ is not smaller than 0·5 but smaller than one. The entry flow in curved pipes can be categorized into the following three cases (for details see Yao 1977):

(i) When both $\bar{\alpha}$ and D are small, the flow is slightly distorted from the entry flow in unheated straight pipes, and the solution can be obtained by perturbing the solution of the developing flow in unheated straight pipes. There are two regions: $O(a)$ and $O(aRe)$. The matched asymptotic solution for the region of $O(a)$ was given by Singh (1974) and breaks down at a distance $O(a/\bar{\alpha}^{\frac{1}{2}})$, corresponding physically to the point beyond which the effect of the centrifugal force, initially small, becomes as important as inertia and viscous forces within the boundary layer. There are two misprints in Singh's paper. The term '$-\cos\sigma s$' in equations (83) and (84) should be replaced by '$1-\cos\sigma s$' in order to satisfy the entry conditions (10) in his paper (see Singh 1974). Also, the matched asymptotic solution developed for the region a distance $O(a)$ apparently breaks down at a distance $O(aRe)$, since aRe is the length scale of the region that flow traverses to the fully developed flow in unheated straight pipes. There are two possible length scales for the region downstream of the region distance $O(a)$ from the entrance. However, $aRe < a/\bar{\alpha}^{\frac{1}{2}}$ when D is small. This suggests that the flow will be fully developed before centrifugal forces lose their secondary role, when D is small.

(ii) When $\bar{\alpha}$ is small and D is large, there are three length scales: a, $a/\bar{\alpha}^{\frac{1}{2}}$, and $aRe/D^{\frac{1}{2}}$. The solutions of regions distances $O(a/\bar{\alpha}^{\frac{1}{2}})$ and $O(aRe/D^{\frac{1}{2}})$ were given by Yao & Berger (1975). The solution of the region a distance $O(aRe/D^{\frac{1}{2}})$ asymptotically approaches the fully developed state (Baura's flow 1963).†

It is interesting to note that the size of the region where Singh's flow is valid depends on the values of $\bar{\alpha}$. It shrinks as the values of $\bar{\alpha}$ increase.

(iii) When both $\bar{\alpha}$ and D are large, the region governed by Singh's flow is shrunk to zero. For this case, the developing flow is governed by the solution presented by Yao & Berger (1975).

† The author wishes to thank the referee for pointing out that Baura's solution is only a crude approximation.

Heated straight pipes

The developing flow in heated straight pipes can be categorized into cases similar to the developing flow in curved pipes.

(i) When ϵ, Gr and $ReGr$ are small, there are two regions: $O(a)$ and $O(aRe)$. The flow deviates slightly from the developing Poiseuille flow.

(ii) When ϵ and Gr are small but $ReGr$ is large, the flow develops similarly to case (i) initially in the region $z \sim O(a)$ and $z \sim O(aRe)$. However, the secondary flow grows further downstream and becomes a dominant component. The axial length scale is not known but may be in the form aRe/Gr^n where n is a constant. The fully developed flow of this case was studied by Mori & Futugami (1967).

(iii) When ϵ is small and Gr is large, the first two regions are $O(a)$ and $O(a/\epsilon^{\frac{2}{5}})$. The flow will approach its fully developed stage in the third region; however, the characteristic length scale of the third region is not known and can only be found from the solution of the second region, $z \sim O(a/\epsilon^{\frac{2}{5}})$, which is not available now.

(iv) When ϵ is large, the region $z \sim O(a)$ does not exist. Besides this, the flow development is similar to case (iii).

The fully developed flows in heated straight pipes under the condition of constant wall heat flux are given by Morton (1959) if $ReRa$ is small and by Mori & Futagami (1967) if $ReRa$ is large. The solution presented in this paper is limited to the region distance $O(a)$ from the inlet for constant wall heat flux conditions. The solution is valid when $\epsilon z^{\frac{2}{5}}$ is less than 0·1 (see Yao, Catton & McDonough 1978).

The physics of the entry flow in a heated straight pipe when ϵ is small and Gr is large can be visualized as in the following.

As the fluid enters the pipe, a boundary layer develops on the wall with a secondary flow developed inside the boundary layer by the buoyancy forces due to the temperature difference between the wall and the inlet fluid. The central inviscid flow will be accelerated by the displacement of the axial boundary layer like that in an unheated straight pipe. This motion generates node-like sinks along the centre-line of the pipe and causes fluid particles to move toward the centre of the pipe. Simultaneously, the displacement of the secondary boundary layer induces a uniform, downward stream on the cross-section of the pipe. The combination of the downward stream with the radial stream responds to the development of two vortices in the central core of the pipe. A saddle-point-like stagnation point, initially coincident with the centre-line, moves downward along the vertical symmetry line of the pipe, and the saddle-point-like stagnation point will stay in the core of the pipe within the region of $O(a)$. The axial velocity profile turns to accommodate the downward stream generated by the displacement of the secondary boundary layer: the component of the axial pressure gradient induced by the secondary flow is negative along the bottom wall of the pipe and is positive along the top wall of the pipe. It is found that the temperature in the central core of the pipe does not change within the region of $O(a)$ and is identical to the inlet temperature.

As the fluid enters the second region, $\bar{z} \sim O(a/\epsilon^{\frac{2}{5}})$, the secondary flow becomes important. The ratio of the secondary-flow velocity and the axial-flow velocity is of the order of ϵ in $z \sim O(a)$ and increases to $\epsilon^{\frac{2}{5}}$ in $z \sim O(a/\epsilon^{\frac{2}{5}})$ (see Yao *et al.* 1978). The interaction of the secondary flow and the axial flow becomes so important that the perturbation solution, $z \sim O(a)$, is not valid any more. No solution is available in the

region $z \sim O(a/\epsilon^{\frac{2}{5}})$. Owing to the similarity between the flow in heated straight pipes and in curved pipes, the physics can be intuitively visualized as in the following. The downward inviscid stream increases and forms a three-dimensional stagnation flow along the bottom wall of the pipe. This stream may prevent the boundary layer from diffusing away; also, the fluid is sucked into the boundary layer in order to maintain the secondary boundary layer. These two mechanisms may cause the boundary layer to thin along the bottom wall of the pipe as the fluid moves downstream. Since the magnitude of the downward stream increases, the temperature of the central core flow gradually increases. The velocity profile of the central inviscid flow also gradually turns to accommodate the increasing downward stream. Since the thickness of the axial boundary layer does not grow very much in this region, the acceleration of the inviscid core flow, due to the displacement effect of the axial boundary layer, also slows down.

The flow approaches its fully developed stage in the region $z \sim O(a/\epsilon^n)$, where $n < \frac{2}{5}$ is not known but can be found from the solution of the region $z \sim O(a/\epsilon^{\frac{2}{5}})$. It is difficult to visualize the flow development in this region, now. However, following the flow development in curved pipes and the experimental evidence of the fully developed flow in heated straight pipes, we might say that a three-dimensional separation starts to occur along the top wall of the pipe. The effect of the boundary-layer separation on the development of the inviscid core flow further complicates the problem. No rigorous solution of the flow development is available now. The study of the flow development in this region is worth while and can shed light on the physics of the flow pattern for a fully developed flow in heated straight pipes where Gr is large as well as for a fully developed flow in curved pipes when D is large.

As the flow approaches its fully developed stage, the difference between the wall temperature and the temperature of the central core approaches a constant. The buoyancy force constantly exists; the secondary flow can increase the heat transfer rate by mixing the fluid in the boundary layer and in the central core. The mixing can, also, stabilize the pipe flow; the transition Reynolds number in heated straight pipes is much higher than that in unheated straight pipes.

The solution in this paper is for the region a distance $O(a)$ from the pipe entrance. The solution is valid when ϵ is small and can be applied to the cases (i), (ii), and (iii). Barker & Jennings (1977) studied the transition of the boundary layer in a heated straight pipe. The inlet condition in their experiment was a uniformly distributed velocity profile. Unfortunately, no instrumentation is allowed to be installed inside the pipe for a high-speed flow transition study. Therefore, we cannot compare our theory with their experiment.

2. Governing equations

Near the inlet it is natural to refer lengths to the radius a of the pipe, and velocities to the uniform inlet velocity W_{in} (figure 1). The pressure is non-dimensionalized by $\rho_{\text{in}} W_{\text{in}}^2$, where ρ_{in} is the density. The dimensionless temperature is defined in terms of the inlet temperature, T_{in}, and the constant wall heat flux, q_w, as

$$\Theta = (T - T_{\text{in}})\, kRe^{\frac{1}{2}}/aq_w.$$

The fluid density variation due to heating is considered only important in the form of the buoyancy forces. This is known as the Boussinesq approximation, which is valid

when the change of the fluid density is small compared with the fluid density. In cylindrical polars the dimensionless equations of motion and energy with the Boussinesq approximation become

$$\frac{1}{r}\frac{\partial(rU)}{\partial r}+\frac{1}{r}\frac{\partial V}{\partial \phi}+\frac{\partial W}{\partial z}=0, \tag{2a}$$

$$U\frac{\partial U}{\partial r}+\frac{V}{r}\frac{\partial U}{\partial \phi}+W\frac{\partial U}{\partial z}-\frac{V^2}{r}=-\frac{\partial P}{\partial r}+\epsilon(\Theta-\Theta_c)\cos\phi+\frac{1}{Re}\left(\nabla^2 U-\frac{U}{r^2}-\frac{2}{r^2}\frac{\partial V}{\partial \phi}\right), \tag{2b}$$

$$U\frac{\partial V}{\partial r}+\frac{V}{r}\frac{\partial V}{\partial \phi}+W\frac{\partial V}{\partial z}+\frac{UV}{r}=-\frac{\partial P}{r\,\partial \phi}+\epsilon(\Theta-\Theta_c)\sin\phi+\frac{1}{Re}\left(\nabla^2\nabla-\frac{V}{r^2}+\frac{2}{r^2}\frac{\partial U}{\partial \phi}\right). \tag{2c}$$

$$U\frac{\partial W}{\partial r}+\frac{V}{r}\frac{\partial W}{\partial \phi}+W\frac{\partial W}{\partial z}=-\frac{\partial P}{\partial z}+\frac{1}{Re}\nabla^2 W, \tag{2d}$$

$$U\frac{\partial \Theta}{\partial r}+\frac{V}{r}\frac{\partial \Theta}{\partial \phi}+W\frac{\partial \Theta}{\partial z}=\frac{1}{Pr\,Re}\nabla^2\Theta, \tag{2e}$$

where

$$\nabla^2=\frac{\partial^2}{\partial r^2}+\frac{1}{r}\frac{\partial}{\partial r}+\frac{1}{r^2}\frac{\partial^2}{\partial \phi^2}+\frac{\partial^2}{\partial z^2} \tag{3}$$

is the Laplace operator, $\Theta_c(z)$ is the temperature along the centre-line of the pipe. The parameters ϵ, Re and Pr are defined in (1).

The entry condition is uniform inlet axial velocity and temperature; the reference pressure at the inlet is set equal to zero. It may be noted that, in the absence of viscosity, the exact solution of (2) satisfying the above inlet condition and slip wall condition is

$$W=1, \quad U=V=P=\Theta=0. \tag{4}$$

3. Solutions

As the fluid flows into the pipe, the viscous forces are confined to the thin boundary layer near the wall of the pipe. For a heated pipe the secondary flow is created by the buoyancy forces inside the thermal boundary layer. The ratio of the thicknesses of the thermal boundary layer to the momentum boundary layer depends on the Prandtl number. Viscous forces and heat conduction can be ignored away from the boundary layer; the flow is isothermal and inviscid in the central core of the pipe. The core flow is accelerated owing to the displacement effect of the boundary layer and fluid particles will be displaced from the wall toward the centre of the pipe. Simultaneously, a downward stream is developed due to the displacement effect of the secondary boundary layer. The combination of the radial-direction motion with the downward one gives the stream pattern of two developing vortices on the cross-section normal to the axis of the pipe. The downward stream will also skew the axial velocity by accelerating it below the centre and decelerating it above the centre of the pipe. The analysis shows that the development of the secondary flow due to the heating effect near the entrance when ϵ is small can be obtained by perturbing the solution of the developing flow in an unheated pipe.

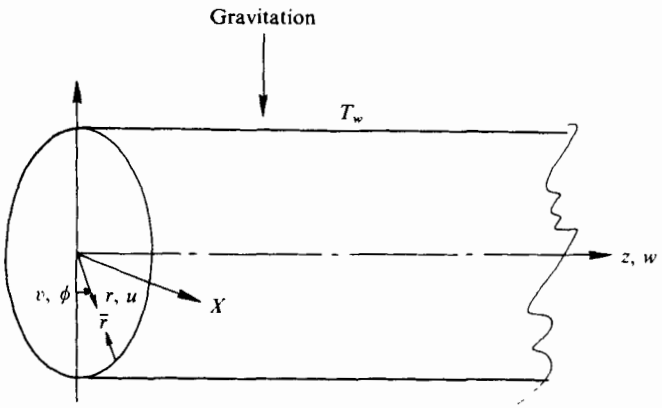

FIGURE 1. Co-ordinate systems.

Zeroth-order solution in the inviscid core

The solution of the inviscid core flow can be obtained by expanding the dependent variables into series

$$\left.\begin{aligned} U &= U_0+\delta U_1+\ldots,\\ V &= V_0+\delta V_1+\ldots,\\ W &= W_0+\delta W_1+\ldots,\\ P &= P_0+\delta P_1+\ldots,\\ \Theta &= \Theta_0+\delta\Theta_1+\ldots,\\ \Theta_c &= \Theta_0^c+\delta\Theta_1^c+\ldots, \end{aligned}\right\} \tag{5}$$

where δ is the expansion parameter and can be determined by matching with the zeroth-order boundary-layer flow. It can be shown that it is equal to $1/Re^{\frac{1}{2}}$. The governing equations of the first order can be obtained by taking the limit of $Re \to \infty$ from (2). The zeroth-order solutions which satisfy the uniform inlet velocity and temperature conditions and the slip condition at the pipe wall are just the undisturbed flow, which is given in (4).

Zeroth-order boundary-layer flow

Near the pipe wall, the viscous forces and heat conduction normal to the wall become important. The radial co-ordinate r is stretched to reflect this physical fact. Accordingly, we introduce the inner variables, as in the classical boundary layer.

$$r = 1-\delta\bar{r}, \quad U = -\delta u, \quad V(r,\phi,z) = v(\bar{r},\phi,z), \quad \text{etc.} \tag{6}$$

Combination of (2) and (6), after neglecting the smaller-order terms, yields

$$\left.\begin{aligned} &\frac{\partial u}{\partial\bar{r}}+\frac{\partial v}{\partial\phi}+\frac{\partial w}{\partial z} = 0,\\ &u\frac{\partial v}{\partial\bar{r}}+v\frac{\partial v}{\partial\phi}+w\frac{\partial v}{\partial z} = -\frac{\partial P}{\partial\phi}+\epsilon(\theta-\theta_c)\sin\phi+\frac{\partial^2 v}{\partial\bar{r}^2},\\ &u\frac{\partial w}{\partial\bar{r}}+v\frac{\partial w}{\partial\phi}+w\frac{\partial w}{\partial z} = -\frac{\partial P}{\partial z}+\frac{\partial^2 w}{\partial\bar{r}^2},\\ &u\frac{\partial\theta}{\partial\bar{r}}+v\frac{\partial\theta}{\partial\phi}+w\frac{\partial\theta}{\partial z} = \frac{1}{Pr}\frac{\partial^2\theta}{\partial\bar{r}^2}. \end{aligned}\right\} \tag{7}$$

Pr	0·01	1·0	10·0
β_1	1·2167	1·2167	1·2167
β_3	23·3511	0·9062	0·1524

TABLE 1. Constants from the computation of the boundary-layer flow.

The associated boundary conditions of (7) are as follows.

$$\left.\begin{array}{lll} \text{At} & z=0, \quad u=v=\theta=0, \quad w=1 & \text{(entrance condition).} \\ \text{At} & \bar{r}=0, \quad u=v=w=0, \quad \theta_{\bar{r}}=-1 & \text{(no-slip condition at wall), (constant wall heat flux).} \\ \text{As} & \bar{r}\to\infty,\ v\to 0,\ w\to 1,\ \theta\to 0 & \text{(matching condition with zeroth-order inviscid core flow).} \end{array}\right\} \tag{8}$$

The dependent variables can be expanded as, when ϵ is small,

$$w = f_0' + \epsilon(2z)^{\frac{1}{2}} F_1' \cos\phi + \ldots, \tag{9a}$$

$$v = \epsilon(2z)^{\frac{1}{2}} F_2' \sin\phi + \ldots, \tag{9b}$$

$$u = \frac{1}{(2z)^{\frac{1}{2}}}(\eta f_0' - f_0) + \epsilon(2z)^2(\eta F_1' - 6F_1 - F_2)\cos\phi + \ldots, \tag{9c}$$

$$\theta = (2z)^{\frac{1}{2}}\theta_0 + \epsilon(2z)^3 G\cos\phi + \ldots. \tag{9d}$$

The functions f_0, F_1, F_2, θ_0 and G depend on η only, where $\eta = r/(2z)^{\frac{1}{2}}$, known as the Blasius variable. The governing equations for f_0, θ_0, F_1, F_2, and G are

$$f_0''' + f_0 f_0'' = 0, \tag{10a}$$

$$\frac{1}{Pr}\theta_0'' + f_0\theta_0' - f_0'\theta_0 = 0, \tag{10b}$$

$$F_1''' + f_0 F_1'' - 5f_0' F_1' + 6f_0'' F_1 = -f_0'' F_2, \tag{10c}$$

$$F_2''' + f_0 F_2'' - 3f_0' F_2' = -\theta_0, \tag{10d}$$

$$\frac{1}{Pr}G'' + f_0 G' - 6f_0' G = -\theta_0 F_1' - \theta_0'(6F_1 - F_2). \tag{10e}$$

The boundary conditions on (10) are

$$\left.\begin{array}{l} f_0 = f_0' = 0, \quad \theta_0' = -1 \quad \text{at} \quad \eta = 0, \\ f_0' \to 1, \quad \theta_0 \to 0 \quad \text{as} \quad \eta \to \infty, \end{array}\right\} \tag{11a}$$

and

$$\left.\begin{array}{l} F_1 = F_1' = F_2 = F_2' = G' = 0 \quad \text{at} \quad \eta = 0, \\ F_1', F_2', G \to 0 \quad \text{as} \quad \eta \to \infty. \end{array}\right\} \tag{11b}$$

The boundary-layer velocity u, normal to the wall along the interface of the boundary layer and the inviscid core flow, is

$$U_1(r=1) = -\frac{\beta_1}{2z^{\frac{1}{2}}} + \beta_3\,\epsilon(2z)^2\cos\phi + \ldots, \tag{12a}$$

where

$$\beta_3 = \lim_{\eta\to\infty}(6F_1 + F_2). \tag{12b}$$

Equation (12a) is the matching condition for the second-order inviscid core flow. The values of β_1 and β_3 for different Prandtl numbers are obtained by the numerical integration of (10) and are listed in table 1.

First-order inviscid core flow

The equations of the first-order inviscid core flow are found by substituting (4) and (5) into (2). They are

$$\frac{1}{r}\frac{\partial(rU_1)}{\partial r}+\frac{1}{r}\frac{\partial V_1}{\partial \phi}+\frac{\partial W_1}{\partial z}=0, \tag{13a}$$

$$\frac{\partial U_1}{\partial z}=-\frac{\partial P_1}{\partial r}+\epsilon(\Theta_1-\Theta_1^c)\cos\phi, \tag{13b}$$

$$\frac{\partial V_1}{\partial z}=-\frac{\partial P_1}{r\partial \phi}+\epsilon(\Theta_1-\Theta_1^c)\sin\phi, \tag{13c}$$

$$\frac{\partial W_1}{\partial z}=-\frac{\partial P_1}{\partial z}, \tag{13d}$$

$$\frac{\partial \Theta_1}{\partial z}=0. \tag{13e}$$

The temperature of the inviscid core flow, up to this order, is still not changed and is equal to the inlet temperature. This is confirmed by (13*e*), the solution of which is $\Theta_1 \equiv 0$. Therefore, there is no buoyancy force acting on the fluid in the central core of the pipe. Equations (13*a*) to (13*d*) can be separated into two parts: the accelerating axial flow due to the displacement effect of axial boundary layer and the downward stream due to the displacement effect of the secondary boundary layer. The equations governing the two phenomena are found by substituting

$$\left.\begin{aligned} U_1 &= U_{10}+\epsilon U_{11}\cos\phi+\ldots,\\ V_1 &= \epsilon V_{11}\sin\phi+\ldots,\\ W_1 &= W_{10}+\epsilon W_{11}\cos\phi+\ldots,\\ P_1 &= P_{10}+\epsilon P_{11}\cos\Phi+\ldots \end{aligned}\right\} \tag{14}$$

into (13) when ϵ is small. After collecting the terms without ϵ and with ϵ, we have

$$\frac{1}{r}\frac{\partial(rU_{10})}{\partial r}+\frac{\partial W_{10}}{\partial z}=0, \tag{15a}$$

$$\frac{\partial U_{10}}{\partial z}=-\frac{\partial P_{10}}{\partial r}, \tag{15b}$$

$$\frac{\partial W_{10}}{\partial z}=-\frac{\partial P_{10}}{\partial z}, \tag{15c}$$

and

$$\frac{1}{r}\frac{\partial(rU_{11})}{\partial r}+\frac{V_{11}}{r}+\frac{\partial W_{11}}{\partial z}=0, \tag{16a}$$

$$\frac{\partial U_{11}}{\partial z}=-\frac{\partial P_{11}}{\partial r}, \tag{16b}$$

$$\frac{\partial V_{11}}{\partial z}=\frac{P_{11}}{r}, \tag{16c}$$

$$\frac{\partial W_{11}}{\partial z}=-\frac{\partial P_{11}}{\partial z}. \tag{16d}$$

Displacement effect, $O(\delta)$. The appropriate matching condition for (15) is

$$U_{10} = -\beta_1/(2z)^{\frac{1}{2}} \quad \text{at} \quad r = 1, \tag{17a}$$

and the entry conditions are

$$P_{10} = W_{10} = 0 \quad \text{at} \quad z = 0. \tag{17b}$$

Integrating (15c) with respect to z and using (17b) gives

$$W_{10} = -P_{10}. \tag{18}$$

Eliminating U_{10} and W_{10} from (15a), (15b), and (18) results in

$$\frac{\partial^2 P_{10}}{\partial r^2} + \frac{1}{r}\frac{\partial P_{10}}{\partial r} + \frac{\partial^2 P_{10}}{\partial z^2} = 0. \tag{19}$$

The solution of (19) satisfying condition (17a) can be found by Fourier transformation in the sense of generalized functions (see Lighthill 1958). It is

$$P_{10} = -\frac{\beta_1}{\pi^{\frac{1}{2}}}\int_0^\infty \alpha^{-\frac{1}{2}}\frac{I_0(\alpha r)}{I_1(\alpha)}\sin\alpha z\, d\alpha, \tag{20a}$$

where I_0 and I_1 are modified Bessel functions.

Substituting (20a) into (15b) and (15c), we obtain

$$W_{10} = \frac{\beta_1}{\pi^{\frac{1}{2}}}\int_0^\infty \alpha^{-\frac{1}{2}}\frac{I_0(\alpha r)}{I_1(\alpha)}\sin\alpha z\, d\alpha, \tag{20b}$$

and

$$U_{10} = \frac{-\beta_1}{\pi^{\frac{1}{2}}}\int_0^\infty \alpha^{-\frac{1}{2}}\frac{I_1(\alpha r)}{I_1(\alpha)}(\cos\alpha z - 1)\, d\alpha. \tag{20c}$$

The asymptotic values of (20) for large z can be easily found:

$$W_{10} = -P_{10} = \beta_1 2(2z)^{\frac{1}{2}}\left[1 + \frac{1}{4}\frac{r^2}{(2z)^2} + \ldots\right], \tag{21a}$$

$$U_{10} = -\beta_1 r\,(2z)^{-\frac{1}{2}}. \tag{21b}$$

Equations (20) or (21) represent the accelerating flow due to the displacement effect of the boundary layer in an unheated pipe.

Secondary displacement effect, $O(\delta\epsilon)$. The appropriate matching condition for (15) is, from (12),

$$\left.\begin{aligned} U_{11} &= \beta_3(2z)^2 \quad \text{at} \quad r = 1, \\ \text{and} \quad P_{11} &= W_{11} = 0 \quad \text{at} \quad z = 0. \end{aligned}\right\} \tag{22a}$$

With conditions (22a), the solutions of (16) are

$$\begin{aligned} W_{11} = -P_{11} &= 32\beta_3\int_0^\infty \alpha^{-1}\frac{I_1(\alpha r)}{I_0(\alpha) + I_2(\alpha)}\delta'(\alpha)\sin\alpha z\, d\alpha \\ &= 4\beta_3 r(2z), \end{aligned} \tag{22b}$$

$$U_{11} = -V_{11} = \beta_3(2z)^2, \tag{22c}$$

where $\delta'(\alpha)$ is the first derivative of the delta function.

The analysis can be extended systematically to obtain higher-order terms of the solution in the boundary layer and the core. The temperature of the central core is not changed up to $O(\delta\epsilon)$; however, the downward convection, $O(\delta\epsilon)$, will carry the hotter

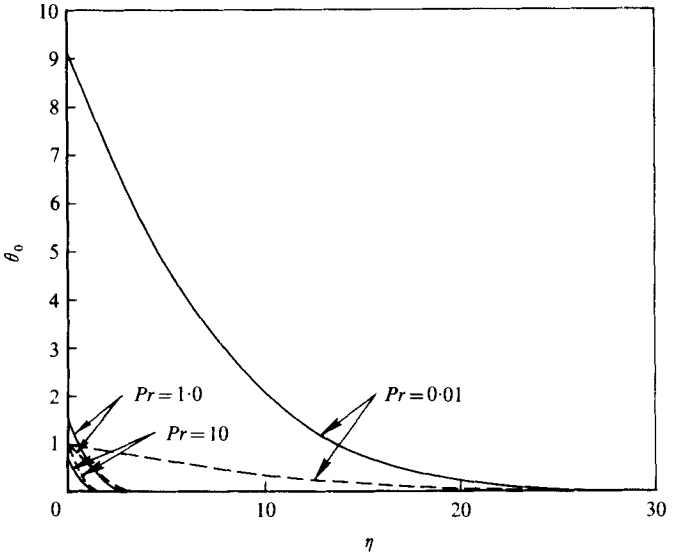

FIGURE 2. First-order temperature θ_0. ——, constant wall temperature; – – – –, constant wall heat flux.

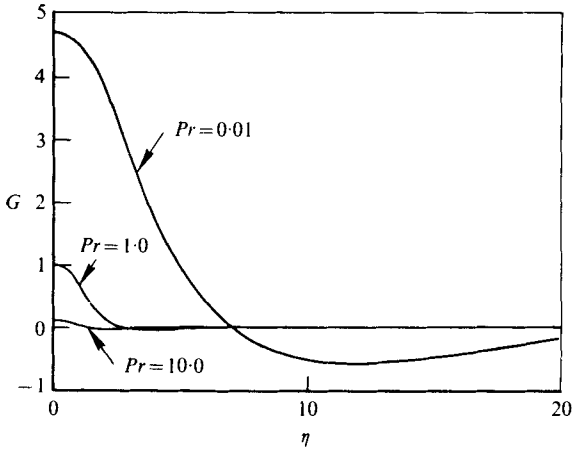

FIGURE 3. Function G.

fluid from the boundary ($-\frac{1}{2}\pi \leqslant \phi \leqslant \frac{1}{2}\pi$) into the cooler core and will increase the temperature of the core flow. The small temperature variation is not considered in this paper.

4. Results and discussion

Boundary-layer flow

The numerical results for the functions θ_0, G, F_1, F_1', F_2, and F_2' are plotted in figures 2–7. The values of θ_0 for the case of constant q_w are larger than those for the case of constant T_w (Yao & Catton 1976, 1977). The wall temperature for the case of constant q_w increases downstream, and its values can be calculated from (9*d*). The

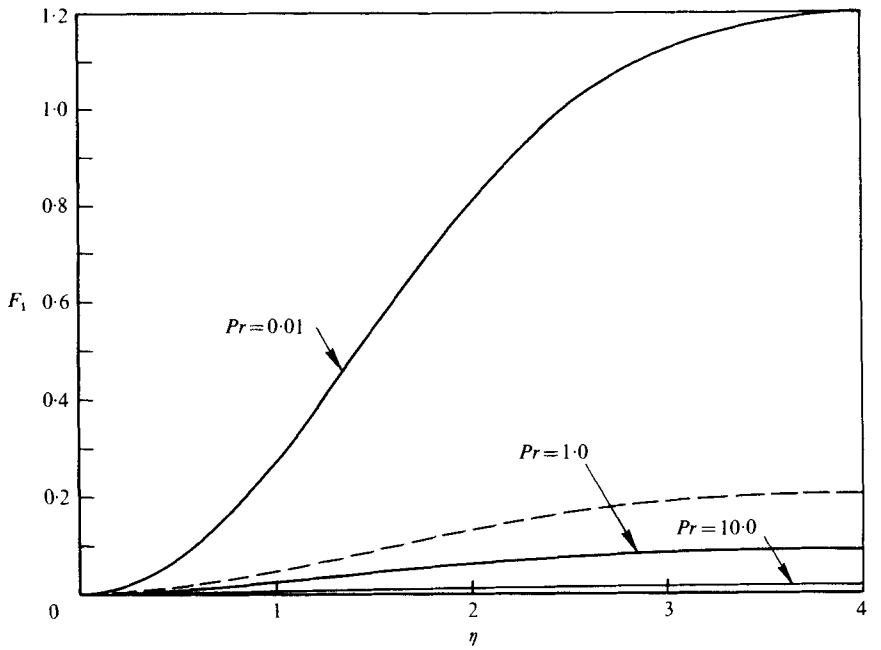

FIGURE 4. Function F_1. ——, constant q_w; – – – –, constant T_w (Pr = 0·01).

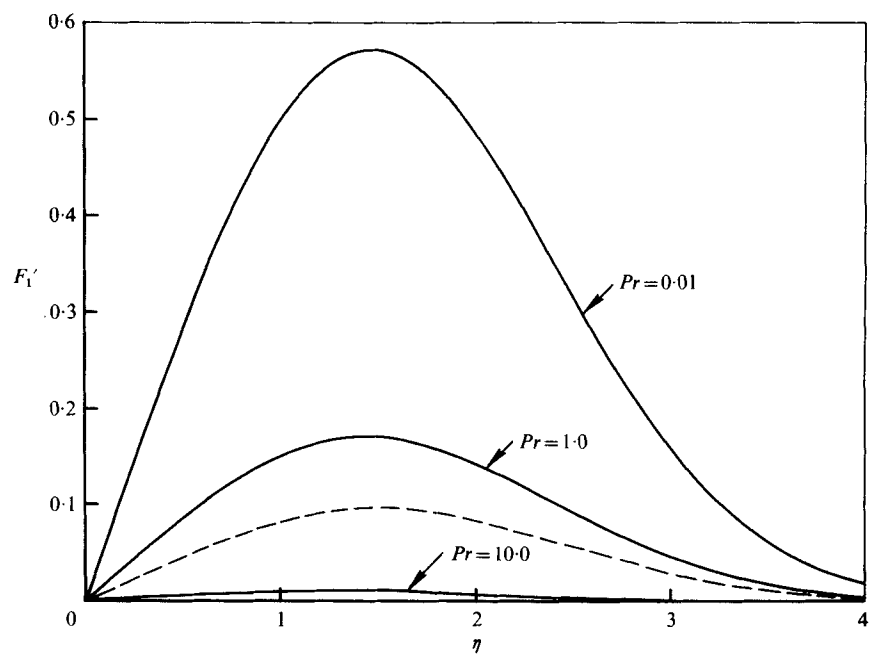

FIGURE 5. Function F_1'. ——, constant q_w; – – – –, constant T_w (Pr = 0·01).

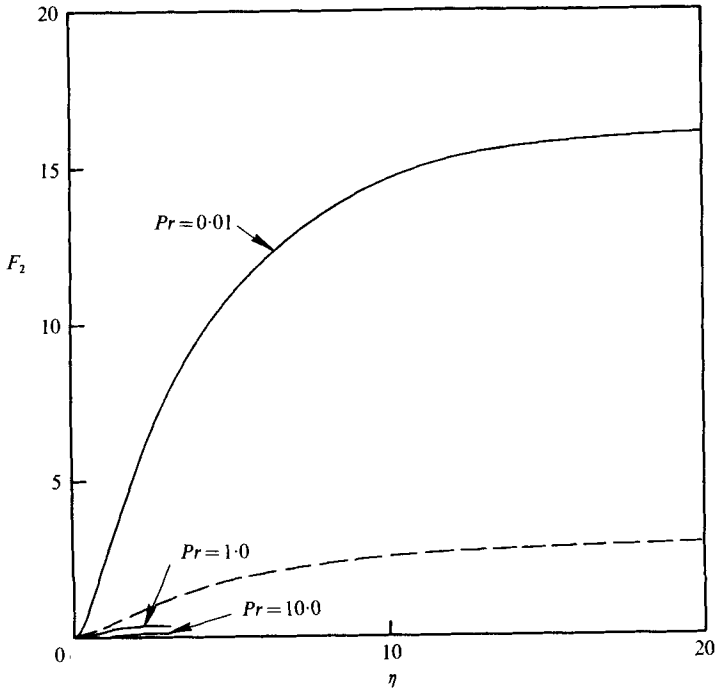

FIGURE 6. Function F_2. ——, constant q_w; – – – –, constant T_w (Pr = 0·01).

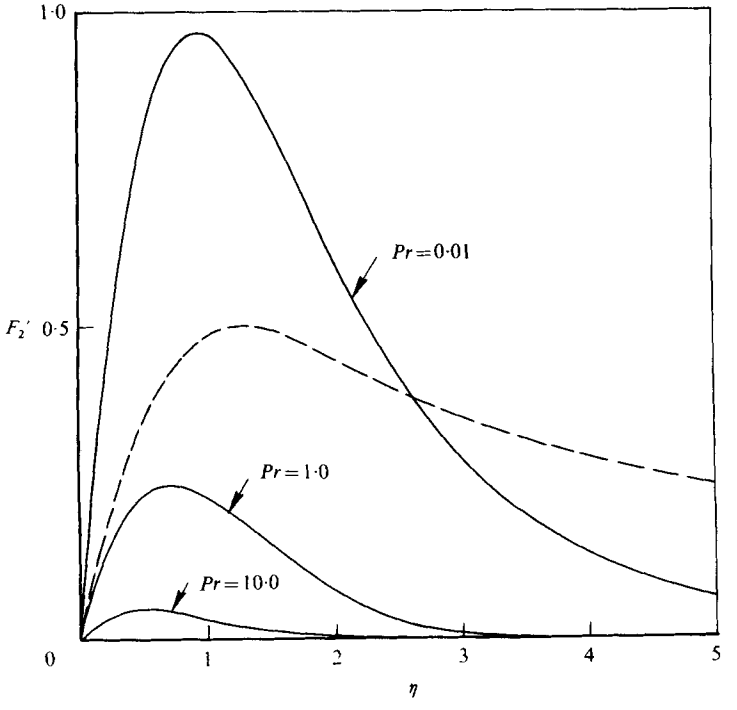

FIGURE 7. Function F_2'. ——, constant q_w; – – – –, constant T_w (Pr = 0·01).

Pr	$\theta_0(0)$	$G(0)$	$F_1''(0)/f_0''(0)$	$F_2''(0)$
0·01	9·1173	4·6807	1·2085	7·1801
1·0	1·5409	1·0053	0·0990	0·7914
10·0	0·7087	0·0958	0·0198	0·2309

TABLE 2. Coefficients for wall temperature and shear stress.

values of θ_0 and G_1 for $Pr = 0{\cdot}01$, 1·0, and 10 are listed in table 2. In figure 3 the values of the perturbed temperature are positive near the wall and negative near the core. The stream function F_1, shown in figure 4, indicates their values are much larger than those for the case of constant T_w. The induced axial velocity profile has more profound effects for the case of constant q_w. Similarly, the buoyancy force induces stronger secondary flow at the constant wall heat flux than at the constant wall temperature shown in figures 6 and 7.

Shear stress

The local shear stress at the wall can be computed from the equation

$$\tau_{rz} = \mu \frac{\partial w}{\partial r}\bigg|_{r=1} \quad \text{and} \quad \tau_{r\phi} = \mu \left(\frac{\partial v}{\partial r}\right)_{r=1}$$

The contribution due to normal velocity gradient is a higher-order effect and is neglected here. Introducing the series expansions (9), the relative importance of the secondary flow on the axial shear stress can be found from

$$\tau_{rz}/(\tau_{rz})_{fc} = 1 + \epsilon(2z)^{\frac{2}{3}}[F_1''(0)/f_0''(0)] \cos\phi + \ldots, \tag{23}$$

where the subscript 'fc' denotes forced convection. The circumferential shear stress can be shown to be proportional to

$$\tau_{r\phi} \sim \epsilon(2z)^{\frac{3}{2}} F_2''(0) \sin\phi. \tag{24}$$

Values of $F_1''(0)/f_0''(0)$ and $F_2''(0)$ are given in table 2. Equations (9d) and (23) indicate that the secondary flow effect on the wall temperature and shear stress grows rapidly downstream, and is proportional to $z^{\frac{1}{2}}$. This means that an initially small secondary effect, which may be treated as a second-order effect in the region a distant $O(a)$ from the inlet, becomes a dominant flow component further downstream.

Inviscid core flow

Equations (20a–c) are numerically integrated by using the fast Fourier transform (for details see Yao 1977). W_{10}/β_1 (or $-P_{10}/\beta_1$) is evaluated at $r = 0{\cdot}5$ as a function of z, and plotted in figure 8. The values of W_{10}/β_1 (or $-P_{10}/\beta_1$) at $r = 0$ differ only slightly from their values at $r = 0{\cdot}5$ and are not presented in figure 8. W_{10} is the flow acceleration due to the displacement effect of the axial boundary layer. The flow is quickly accelerated near the entrance and the acceleration declines and is proportional to $z^{-\frac{1}{2}}$ downstream. The distributions of W_{10} (or P_{10}) on the cross-section normal to the pipe axis are given in figure 9. Near the entrance, $z = 0{\cdot}1$, the axial velocity is higher close to the boundary layer than along the centre-line of the pipe. The delay of the flow acceleration near the centre-line causes the axial velocity profile to become concave. The velocity profile has its maximum velocity off the centre-line. The peaks are

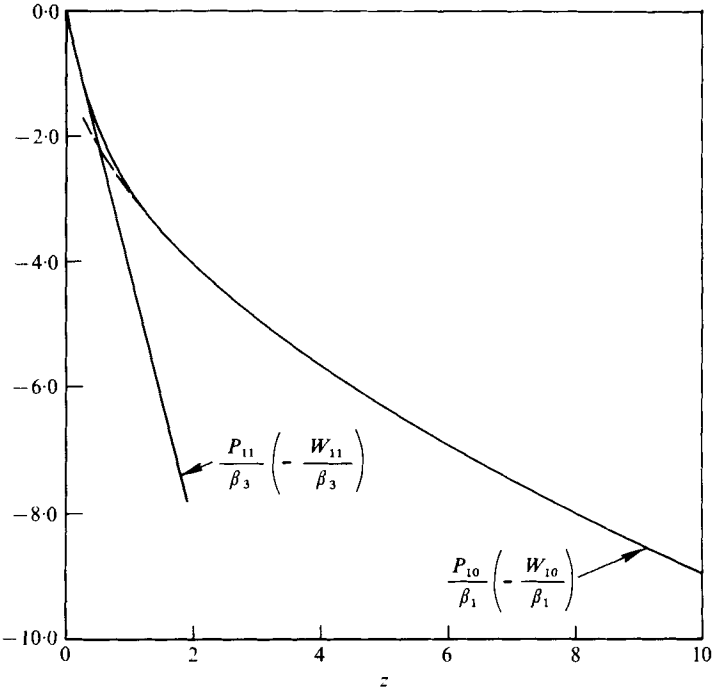

FIGURE 8. Displacement effect W_{10}/β_1 (or $-P_{10}/\beta_1$). $r/a = 0{\cdot}5$. – – – –, asymptotic expansion for large values of z [equation (21)].

eroded downstream and eventually disappear at $z = 2{\cdot}5$ (see figure 8). A similar interpretation can be given to P_{10}, which is the pressure drop.

The displacement effects of the secondary boundary layer are represented by functions W_{11} and P_{11}. Physically, the secondary boundary layer causes the axial flow to turn anticlockwise around the horizontal line passing through the centre of the pipe and normal to the axis of the pipe, $Y = r\cos\phi = 0$, and does not cause any net mean acceleration of the flow.

The comparison of the asymptotic expansions with the exact evaluation of the sine integrals suggests that simpler asymptotic expansions can be used for practical application when z is larger than 2·5, which will cover most ranges of practical interest when ϵ is small. The velocity components and the pressure, in their asymptotic forms, are

$$P = -\delta(2z)^{\frac{1}{2}}2\beta_1\left[1+\frac{r^2(2z)^{-2}}{4}+\ldots\right]-\delta\epsilon 4\beta_3 r(2z)\cos\phi, \tag{25a}$$

$$W = 1-P, \tag{25b}$$

$$U = -\delta\{\beta_1[r(2z)^{-\frac{1}{2}}+\ldots]-\epsilon\beta_3[(2z)^2\cos\phi+\ldots]\}, \tag{25c}$$

$$V = -\delta\epsilon\beta_2[(2z)^2\sin\phi+\ldots]. \tag{25d}$$

Pressure drop

The pressure head will drop along the pipe when the flow is accelerated. The first term of (25a) represents the pressure drop in an unheated pipe due to the displacement of the axial boundary layer. The pressure drops faster close to the edge of the boundary

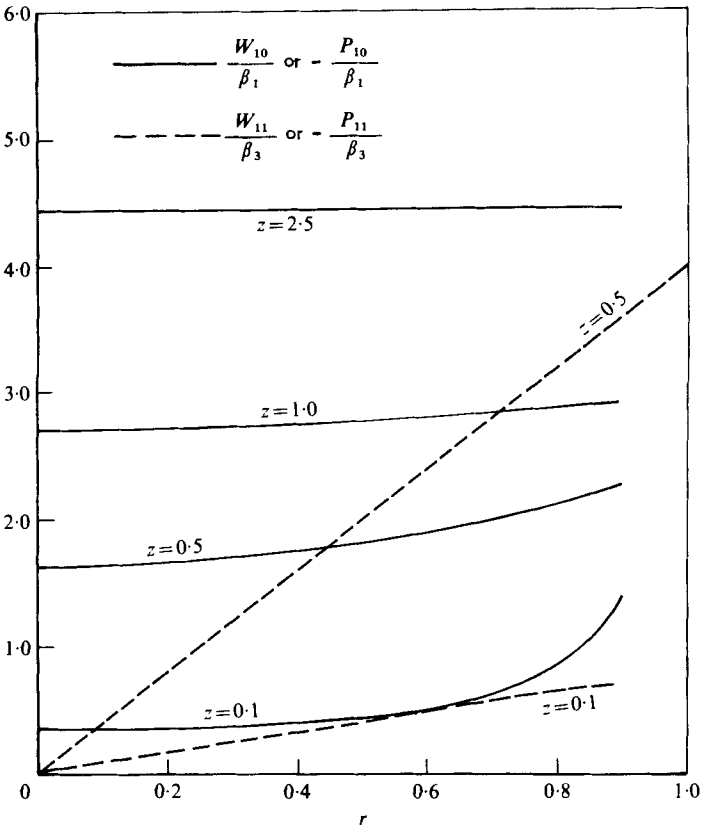

FIGURE 9. Displacement effect: pressure P_{10}/β_1, velocity W_{10}/β_1 on the cross-sections at $z = 0{\cdot}1$, $0{\cdot}5$, $1{\cdot}0$, $2{\cdot}5$. ——, W_{10}/β_1 or $-P_{10}/\beta_1$; – – – –, W_{11}/β_3 or $-P_{11}/\beta_3$.

layer than along the centre-line of the pipe where $r = 0$. The difference in the pressure distribution on the cross-section of the pipe disappears for large z, and the pressure distribution approaches

$$P \sim -\delta 2\beta_1(2z)^{\frac{1}{2}}. \tag{26}$$

The pressure distribution is disturbed when the pipe wall is heated, which is represented by the second term of $(25a)$. This term can be rewritten in $(\bar{X}, \bar{Y}, z)$ co-ordinates as $\delta\epsilon 8\beta_3 Yz$, which shows that the displacement effect of the secondary boundary layer introduces an unfavourable pressure gradient over the upper half of the pipe flow, $Y > 0$, and a favourable one over the lower half of the pipe, $Y < 0$.

Axial-velocity profiles of the core flow

The axial velocity of the core flow can be viewed as a superposition of these components. The first one is the undisturbed flow at the inlet, i.e. $W = 1$. The second one is the accelerated flow due to the displacement effect of the axial boundary layer in an unheated pipe. The last component is due to the displacement of the secondary boundary layer. Similar to the pressure distribution, the third term in (X, Y, z) co-ordinates is $-\delta\epsilon 8\beta_3 Yz$, which means that the axial velocity profile turns anti-clockwise around $Y = 0$. In the region of $z \sim O(a)$, both the second and the third term

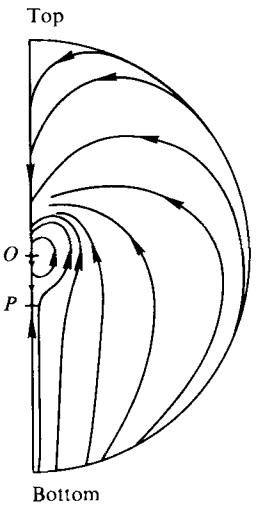

FIGURE 10. Streamlines on the cross-section.

increase as z. However, the second term may be dropped when the third term is still growing downstream beyond the region of $O(a)$ when Gr is not small. For the cases of small Gr (or $Re\,Gr$), the second and the third terms will continue growing until the flow approaches its fully developed state.

Velocities on the cross-section

The radial velocity component U is given in (25c). The first term is due to the displacement effect of the axial boundary layer, which displaces the fluid away from the wall and toward the centre of the pipe. The second term represents the motion when the fluid leaves the boundary layer over the upper half of the pipe ($\frac{1}{2}\pi < \phi < \frac{3}{2}\pi$), and enters the boundary layer over the lower half of the pipe ($-\frac{1}{2}\pi < \phi < \frac{1}{2}\pi$). The first kind of motion declines downstream, and the second one increases owing to heating. They become the same order of magnitude when $z \sim O(a/\epsilon^{\frac{2}{5}})$. Beyond this point, the analysis is not valid any more. For the case of large Gr, the second term becomes dominant and the axial length scale will be $a/\epsilon^{\frac{2}{5}}$. For a small Gr, $a/\epsilon^{\frac{2}{5}}$ is larger than $a\,Re$. This suggests that the next length scale will be $a\,Re$; physically, it suggests that the flow development will be similar to the unheated straight pipe and the solution of the slightly heated pipe can be obtained by perturbing the solution of an unheated pipe. Along the line $\phi = 0$, where $V = 0$, there is a stagnation point at

$$r = (\beta_3/\beta_1)\,[\epsilon(2z)^{\frac{1}{2}}]. \tag{27}$$

This is also a saddle point, point P in figure 10, which is similar to the entry flow of a curved pipe found by Singh (1974). In a heated pipe $\epsilon\beta_3/\beta_1$ is smaller than one (table 1) and the analysis requires the quantity $[\epsilon(2z)^2]$ to be smaller than one. Therefore, the saddle point P can never move into the boundary layer within the region of $O(a)$.

Equation (25d) shows that the circumferential velocity has a maximum at $\phi = \frac{1}{2}\pi$ and is equal to zero at both the top and the bottom of the pipe, $\phi = 0, \pi$.

Streamlines on the cross-section

The projection of the streamlines on a cross-section can be computed by

$$\frac{1}{r}\frac{dr}{d\phi} = \frac{\beta_1 r(2z)^{-\frac{1}{2}} - \epsilon\beta_3 \cos\phi(2z)^2}{\epsilon\beta_3 \sin\phi(2z)^2}. \tag{28}$$

Equation (28) shows that all streamlines are tangential to the vertical line, $\phi = 0, \pi$; they are plotted in figure 10. If z is not too large, the second term in the numerator of (28) can be neglected and (28) can be integrated to give

$$\tan\frac{\phi}{2} = \exp\left[-\frac{\epsilon\beta_3(2z)^{\frac{5}{2}}}{\beta_1 r}\right] + \text{constant}. \tag{29}$$

For $\epsilon = 0$, an unheated straight pipe, (29) becomes $\phi =$ constant. The streamlines on the cross-section are radial straight lines. Within the limit of the analysis, the second term in the numerator of (28) can never be larger than the first one. Nevertheless, stretching somewhat our interpretation of (28) and considering it for large z can predict what may occur for the flow development further downstream. Equation (28) becomes, after neglecting the first term of the numerator and integrating,

$$\bar{x} = \text{constant}, \tag{30}$$

which shows that the streamlines on the cross-section, owing to the displacement effect of the secondary boundary layer, are vertical straight lines. The magnitude of the downward flow is

$$(U_{11}^2 + V_{11}^2)^{\frac{1}{2}} = \beta_3(2z)^2, \tag{31}$$

which increases downstream. This flow, when Gr is large, will eventually become the dominant flow pattern, which is observed by Mori & Futagami (1967). Also, the downward stream forms a stagnation-like flow locally along the bottom wall of the pipe. The convective effect of this locally stagnant flow prevents the boundary layer from growing. Thus, the boundary layer will remain thin as the flow moves downstream. Therefore, the flow acceleration due to the displacement effect of the axial boundary layer will fade out. This suggests that the flow development in the region of $O(a/\epsilon^{\frac{2}{5}})$ is mainly a change in the slope of the axial velocity profile to balance the gradually enhanced flow in the secondary boundary layer. Also, the less favourable pressure gradient near the top wall of the pipe may become an unfavourable pressure gradient. This may be the reason why the separation of the boundary layer occurs further downstream as observed by Mori & Futagami. The downstream solutions are not available, but are needed in order to understand the detailed mechanism of the flow separation along the top wall of a heated straight pipe.

REFERENCES

AGRAWAL, Y., TALBOT, L. & GONG, K. 1978 Laser anemometer study of flow development in curved circular pipes. *J. Fluid Mech.* **85**, 497-518.

BARKER, S. J. & JENNINGS, C. G. 1977 The effect of wall heating on transition in water boundary layers. *AGARD Symposium on Laminar Turbulent Transition*, Copenhagen, Denmark, 2–4 May 1977.

BARUA, S. N. 1963 Secondary flow in stationary curved pipes. *Quart. J. Mech. Appl. Math.* **16**, 61–77.

DEAN, W. R. 1927 Note on the motion of fluid in a curved pipe. *Phil. Mag.* **4**, 208–223.

DEAN, W. R. 1928 The stream-line motion of fluid in a curved pipe. *Phil. Mag.* **5**, 673–695.

ITO, H. 1961 Pressure losses in smooth pipe bends. *Rep. Inst. High Sp. Mech., Japan* **12** (112), 41–62.

LIGHTHILL, M. J. 1958 *Introduction to Fourier Analysis and Generalised Functions.* Cambridge University Press.

MORI, Y. & FUTAGAMI, K. 1967 Forced convective heat transfer in uniformly heated horizontal tubes. *Int. J. Heat Mass Transfer* **10**, 1801–1813.

MORTON, B. R. 1959 Laminar convection in uniformly heated horizontal pipes at low Rayleigh numbers. *Quart. J. Mech. Appl. Math.* **12**, 410–420.

SINGH, M. P. 1974 Entry flow in a curved pipe. *J. Fluid Mech.* **65**, 517–539.

SMITH, F. T. 1976 *Proc. Roy. Soc.* A **351**, 71–87.

VAN DYKE, M. D. 1970 Entry flow in a channel. *J. Fluid Mech.* **44**, 813–823.

WILSON, S. D. R. 1971 Entry flow in a channel. Part 2. *J. Fluid Mech.* **46**, 787–799.

YAO, L.-S. 1977 *Entry Flow in a Heated Tube.* The Rand Corporation, R-2111-ARPA.

YAO, L.-S. & BERGER, S. A. 1975 Entry flow in a curved pipe. *J. Fluid Mech.* **67**, 177–196.

YAO, L.-S. & CATTON, I. 1976 *The Buoyancy and Variable Viscosity Effects on a Water Laminar Boundary Layer Along a Heated Longitudinal Horizontal Cylinder.* The Rand Corporation, R-1966-ARPA.

YAO, L.-S. & CATTON, I. 1977 Buoyancy cross-flow effects on longitudinal boundary layer flow of a heated horizontal hollow cylinder. *J. Heat Transfer, Trans. A.S.M.E.* C **99**, 122–124. (See also The Rand Corporation, R-1907-ARPA, 1976.)

YAO, L.-S., CATTON, I. & MCDONOUGH, J. M. 1978 Free-forced convection from a heated longitudinal horizontal cylinder. *Numerical Heat Transfer* (in the Press).